

PAPER • OPEN ACCESS

Zonal RANS-IDDES and RANS computations of turbulent wake exposed to adverse pressure gradient

Recent citations

- [Numerical simulation of a turbulent wake subjected to adverse pressure gradient](#)
E K Guseva *et al*

To cite this article: E K Guseva *et al* 2018 *J. Phys.: Conf. Ser.* **1135** 012092

View the [article online](#) for updates and enhancements.



IOP | ebooks™

Bringing you innovative digital publishing with leading voices to create your essential collection of books in STEM research.

Start exploring the collection - download the first chapter of every title for free.

Zonal RANS-IDDES and RANS computations of turbulent wake exposed to adverse pressure gradient

E K Guseva¹, M Kh Strelets¹, A K Travin¹, M Burnazzi², T Knopp²

¹Peter the Great St. Petersburg Polytechnic University (SPBPU), Polytechnicheskaya Str. 29, 195251 St. Petersburg, Russia.

²Deutsches Zentrum für Luft- und Raumfahrt e.V. (DLR), Bunsenstr. 10, 37073 Göttingen, Germany

E-mail: katia.guseva@inbox.ru

Abstract. Results are presented of scale-resolving Zonal RANS-IDDES and pure RANS computations of a turbulent wake exposed to adverse pressure gradient. The RANS-IDDES is performed with the use of the NTS code of SPBPU, and the RANS computations are carried with the use of the TAU code of DLR. It is shown that none of the considered RANS models (two linear eddy viscosity models and a full differential Reynolds stress transport model) is capable of reproducing the mean wake characteristics and turbulent statistics predicted by the RANS-IDDES. Accumulated RANS-IDDES database may be used for improvements of RANS models.

1. Introduction

Turbulent wakes exposed to Adverse Pressure Gradient (APG) are a common feature of high-lift wing flows near the maximum lift conditions, when wakes of the upstream elements of the wing are subjected to APG created by downstream elements. Hence accurate prediction of such wakes is of great practical importance. However, reliability and maturity of Reynolds Averaged Navier-Stokes (RANS) computations of high-lift systems at low-speed has not yet been achieved [1], which is to a large extent explained exactly by inability of available RANS models to predict major characteristics of the near wakes in APG. The latter is clearly demonstrated by studies [2-4], which indicate, in particular, that the existing linear eddy-viscosity models, as well as more sophisticated Reynolds Stress Transport models, significantly underpredict the tendency for flow reversal (so-called off-surface separation) due to APG observed in the experiments. However the role of modeling details responsible for this remains unclear since the experimental data are not detailed enough to study the streamwise evolution of the terms of the Reynolds stress transport equation in the near wake region. This motivates further careful experimental studies and Scale-Resolving Simulations (SRS) of the wake in APG flows, which can help to elucidate concrete mechanisms standing behind the failure of the currently available RANS models and, ultimately, to propose corresponding improvements.

These considerations motivated a joint German-Russian project “Wake flows in Adverse Pressure Gradient” (DFG and RBRF Grants No. RA 595/26-1 and 17-58-12002) launched in 2017 and including a new experimental campaign parallel with SRS and RANS computations of wakes in APG. The present paper outlines first results of this project, which confirm the weaknesses of RANS models known from the literature and demonstrate feasibility and a high potential of the scale-resolving approach based on the zonal hybrid RANS-IDDES [5, 6] in terms of capability of providing reliable



and detailed information needed for building enhanced RANS models. This includes quantitative data on the tensor of viscous dissipation ε_{ij} , which is a key term of the Reynolds stress transport RANS models but is out of reach in experiments.

The rest of the paper is organized as follows. We start from a brief description of the computed wake flow (Section 2). In Section 3 an overview is given of the RANS-IDDES and pure RANS approaches used for turbulence representation. Then, Section 4 provides some details on the computational problem statements and numerical aspects of the computations, and Section 5 presents major results of these computations. Finally, in the last Section 6, some conclusions are formulated.

2. Model flow description

The considered model flow is that studied in the experiment of Driver and Mateer [2] (see Fig.1).

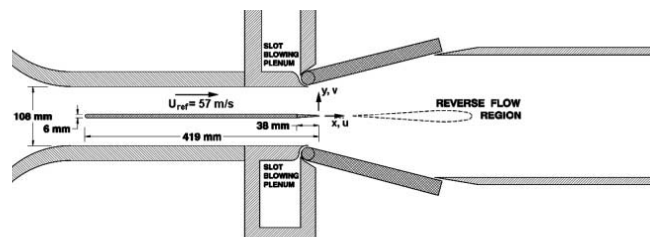


Figure 1. Geometry of test section used in experiments [2]

The experimental setup included the splitter plate with a rounded leading edge and sharp trailing edge (the plate length is 419 mm and its thickness, h , is 6 mm), diffuser with straight walls and variable angle, and a straight duct downstream of the diffuser. Measurements were performed for 4 diffuser angles ensuring its different expansion ratios (ER). One of these values (ER=2.25) corresponding to forming of a relatively small reversed flow region, while keeping two-dimensionality of the mean flow in the experiment, was adopted in the computations. The Mach number in the wind-tunnel was constant and equal to 0.175 and the Reynolds number based on plate length was 10^7 .

It should be noted that in order to prevent separation of the boundary layer from the diffuser walls, blowing slots were incorporated into all the four walls at the entrance to the diffuser. The jets issued from slots had nearly sonic velocity and momentum sufficient to keep the boundary layers attached at all studied diffuser angles. However, considering that no measurements of the jet characteristics were performed, a representation of the experimental setup in CFD appeared to be impossible. So the flow is considered just a reference (no comparisons with the experimental data is performed).

3. Overview of turbulence treatment approaches

As mentioned in the Introduction, two approaches used for turbulence representation in the considered flow are a scale-resolving zonal hybrid approach RANS-IDDES [5, 6] and the conventional RANS approach with different turbulence models.

The hybrid RANS-IDDES approach employs the two-equation $k-\omega$ SST RANS model of Menter [7] in the RANS sub-domain located 100 mm upstream of the trailing edge of the splitter plate and a SRS model IDDES based on the same underlying RANS model in the rest (downstream) part of the computational domain (see a sketch of the computational domain in Fig. 2). At the RANS-IDDES interface the Volume Synthetic Turbulence Generator (VSTG) is applied, which ensures functioning of the IDDES in the Wall-Modelled LES (WMLES) mode (see [6, 8] for details).

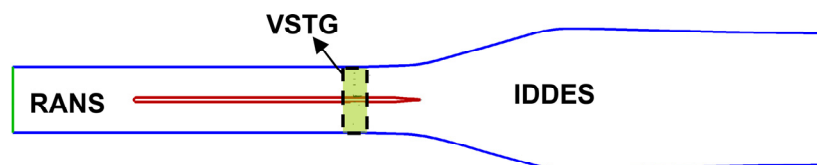


Figure 2. Sketch of computational domain and RANS and IDDES sub-domains

For the pure (in the entire domain) RANS computations, along with the $k-\omega$ SST model, two other models were used, namely, a modification [9] of the one-equation model of Spalart and Allmaras (SA-neg model), and a full differential Reynolds Stress Transport model SSG/LRR- ω [10].

4. Computational problems setups and numerical aspects of the computations

Naturally, computational problem setups and numerics used in the RANS-IDDES and RANS computations are different.

First of all, in the framework of the RANS-IDDES the flow is considered as unsteady and 3D, the span size of the domain is set equal to 0.03 m ($5h$), and spanwise periodicity is assumed, whereas in RANS computations the steady 2D problem statement is used.

The computational domain in XY -plane in both RANS and RANS-IDDES is the same (within RANS-IDDES it is just extruded in the z -direction). The side boundaries of the domain (blue lines in Fig. 2) correspond to an extended mean flow streamlines from the experiment [2], and the inflow and outflow boundaries (green and red lines) are located at $x=0.6$ m upstream and downstream of the trailing edge of the splitter plate ($x=0$), respectively.

Within the zonal RANS-IDDES, the RANS sub-domain extends from the inflow of the domain down to $x=-0.1$ m, and the IDDES sub-domain covers the rest of the plate, where it functions in WMLES mode, and extends up to $x=0.6$ m (downstream of the plate trailing edge it functions as a pure LES). Corresponding computations were performed with the use of the incompressible branch of the SPBPU in-house code NTS [11] (the incompressibility assumption allowing a considerable reduction of resources needed for the rather expensive SRS is quite justified at the considered low Mach number). NTS is a cell-vertex finite-volume code accepting structured multi-block overset grids of Chimera type. Its incompressible branch employs flux-difference splitting method of Rogers and Kwak. In the RANS sub-domain the inviscid fluxes are approximated with the use of a 3rd-order upwind-biased scheme and in the IDDES sub-domain a 4th-order central scheme is adopted. The viscous fluxes are approximated with the 2nd-order central scheme in both sub-domains. For the time integration, an implicit 2nd-order backward Euler scheme with sub-iterations is applied. The boundary conditions used in these simulations are as follows. On the splitter plate no-slip conditions are imposed. At the inflow boundary a uniform velocity is specified and at the outflow boundary a constant pressure is imposed. Finally, at the side boundaries slip conditions are used.

The 2D steady RANS computations were performed with the TAU code of DLR [12]. This is an unstructured code, in which the inviscid fluxes are approximated with the 2nd-order central scheme combined with a matrix artificial dissipation based on 4th-order differences and low Mach-number preconditioning, and the viscous fluxes are treated with the use of 2nd-order upwind Roe scheme. For the time integration, a 2nd-order dual (with sub-iterations) time stepping scheme is used with semi-implicit backward-Euler LUSGS scheme for the inner loops.

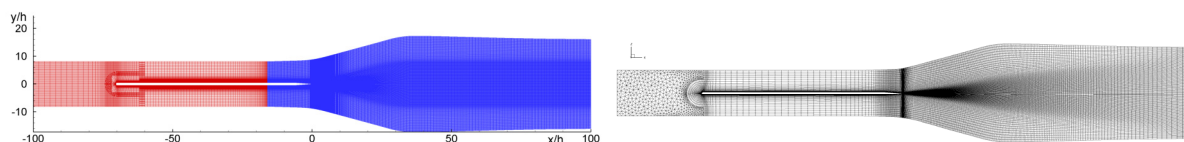


Figure 3. Typical grids used in RANS-IDDES (left) and RANS (right) computations

Typical grids used in the RANS-IDDES and RANS computations are shown in Fig.3. Note that within both approaches grid-sensitivity studies were performed. For the former, their results are discussed in the next section and for the latter only grid-independent results are presented, which were obtained on the grid with 570,000 nodes.

5. Results and Discussion

Considering the primary objective of the study (getting a reliable prediction of the mean flow characteristics and turbulent statistics needed for improvement of RANS models based on SRS) we first dwell upon results of the grid-sensitivity study carried out for RANS-IDDES. They are illustrated

by Figs. 4, 5 which show some results of simulations carried out on three different grids: “coarse”, containing 18 million cells (grid 1), “medium”, containing 28 million cells (grid 2), and “fine”, containing 48 million cells (grid 3).

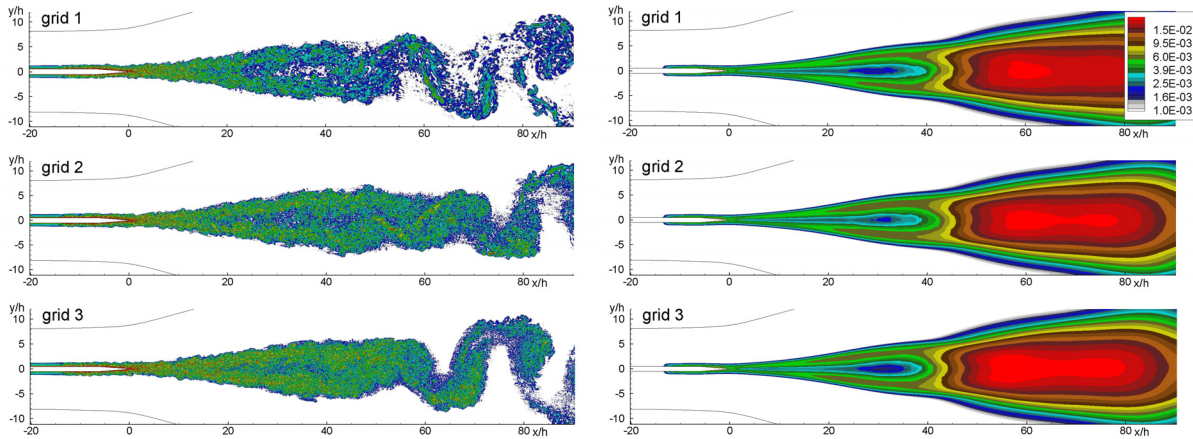


Figure 4. Effect of grid in RANS-IDDES: Snapshots of vorticity magnitude (left) and fields of resolved turbulent kinetic energy (right)

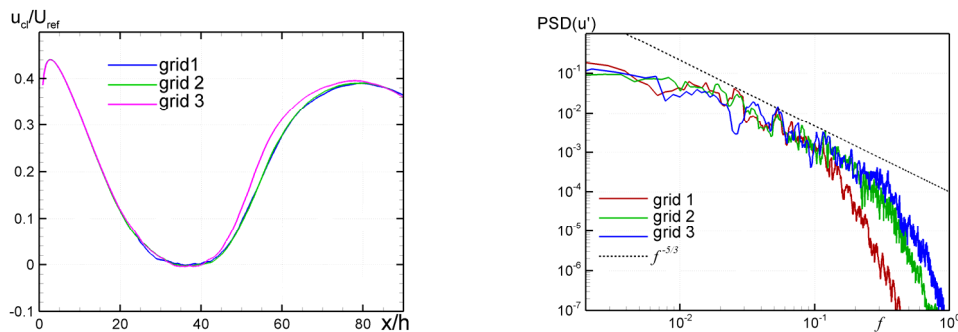


Figure 5. Effect of grid on RANS-IDDES predictions of the mean streamwise velocity and PSD spectra of its fluctuations in the wake symmetry plane

The figures visibly reveal increase of resolution with grid-refinement, with size of smallest resolved eddies consistent with the grid used (Fig. 4a) and increase of the extent of the inertial range of the spectra from about 1 up to nearly 2 decades (Fig. 5b). At the same time, as seen in Figs. 4b and 5a, the effect of the grid-refinement on the mean velocity and turbulent kinetic energy is marginal (same is true for other mean flow characteristics and Reynolds stresses). All these trends suggest plausible LES behavior and its high quality. However, as could be expected considering that even the finest grid spacing Δ is far larger than the Kolmogorov viscous length scale η ($\Delta/\eta > 50$), the viscous dissipation rate directly computed as $\varepsilon \equiv 2\nu \langle S'_{ij} S'_{ij} \rangle$, where S'_{ij} are the elements of fluctuating strain tensor ($S'_{ij} = 0.5(\partial u'_i / \partial x_j + \partial u'_j / \partial x_i)$), turns out to be very sensitive to grid. Moreover, a comparison of the ε -fields computed on the three considered grids (not shown) does not reveal any trend to saturation with the grid-refinement. So, for computing the viscous dissipation rate an alternative approach proposed by Dejoan and Leschziner [13] was applied, which is based on the balance of the terms in the Reynolds stress transport equations. Corresponding (computed with the use of this approach) fields of ε and profiles of ε_{ij} are presented in Fig. 6. One can see that the approach [13] allows getting virtually grid-independent fields of these quantities even on the medium grid (grid 2) with the step size in the focus region of IDDES about 75 Kolmogorov length scales.

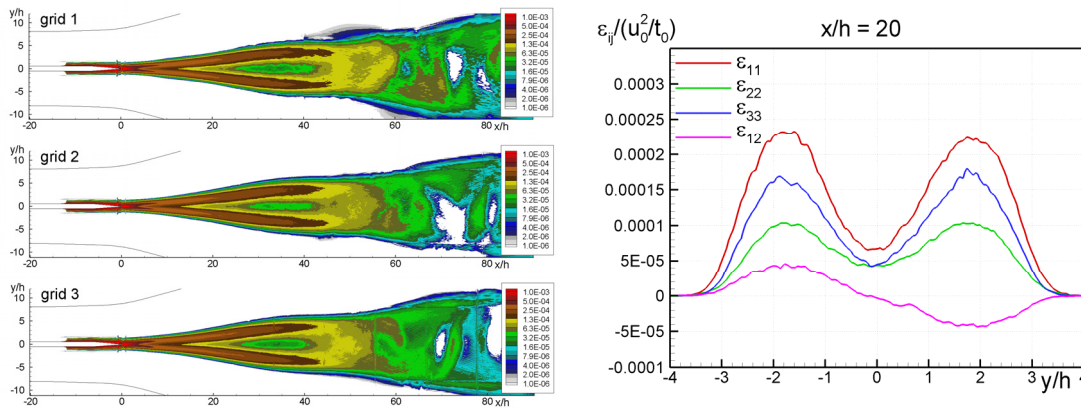


Figure 6. Contours of viscous dissipation rate from RANS-IDDES and profiles of different components of the dissipation rate tensor computed with the use of approach [13]

Note in conclusion that, as seen in Fig.4 above, at $x/h > \sim 45$ ($x > \sim 0.3m$) the simulations predict global oscillations of the wake and formation of large coherent structures, which cannot be captured by any steady RANS model (exactly these oscillations cause a rapid increase of the turbulent kinetic energy in this region).

Because of the space limit, we are not able to present a systematic comparison of the RANS-IDDES predictions outlined above with corresponding RANS solutions obtained with the use of the considered turbulence models and show in Figs. 7, 8 only a restricted but still representative comparison of the two approaches.

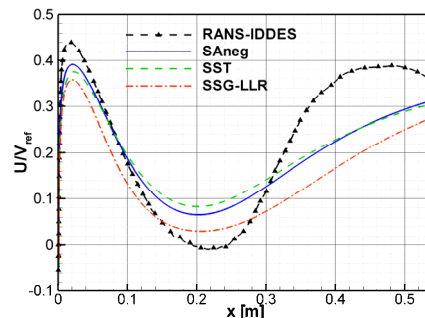


Figure 7. Comparison of distributions of streamwise velocity component along the wake symmetry plane predicted by RANS-IDDES and by three considered RANS models

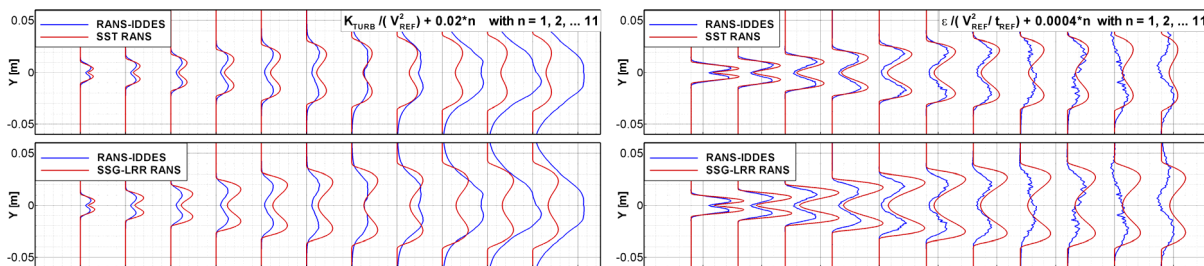


Figure 8. Comparison of profiles of kinetic energy and dissipation rate in wake sections $x=x_n$ predicted by RANS-IDDES and by SST and SSG-LLR RANS ($x_1/h=10, \Delta x/h=5$)

Analysis of these figures suggests that the RANS models are not capable of providing sufficient accuracy not only in the region of the global wake oscillation ($x/h > \sim 45$), which, as mentioned above, is quite natural, but also at $x/h < 45$, where the wake remains globally stable. In particular, in this region all the RANS models considerably underpredict the velocity deficit caused by APG (see Fig. 7) and fail to reproduce the behavior of the profiles of the turbulent kinetic energy and its viscous

dissipation rate (Fig.8), thus supporting conclusions of the previous studies regarding the poor performance of the existing RANS models for the wake in APG flows.

6. Conclusions and outlook

Results are presented of detailed SRS (zonal RANS-IDDES) of the flat plate wake subjected to APG created by a plane diffuser. Analysis of these simulations suggests that the RANS-IDDES approach is quite capable of ensuring a reliable prediction of both major mean flow characteristics and turbulent statistics, including the viscous dissipation rate, on quite modest computational grids of around 20 million cells. The latter turned out possible thanks to the use of the efficient post-processing approach proposed by Dejoan and Leschziner (2005).

Along with this, 2D steady RANS computations of the same flow are carried out with the use of both linear eddy-viscosity and Reynolds Stress models. A comparison of the results of SRS and RANS computations shows that the RANS models are not capable of accurate prediction of the flow in question, thus clearly demonstrating a need for their further enhancement based on the detailed information provided by the SRS. Achieving this would allow using RANS-based computations as an integrated part of wing design not only for cruise flight but also for high-lift low-speed regimes.

Acknowledgements

The study was funded by DFG and RBRF (Grants No. RA 595/26-1 and No. 17-58-12002). RANS-IDDES computations were performed with the use of resources of the Supercomputer Center "Polytechnicheskyy".

References

- [1] Rumsey, C.L., Ying, S.X. 2002. Prediction of high lift: review of present CFD capability. *Progress in Aerospace Sciences*, **38**,145-180.
- [2] Driver, D.M., Mateer, G.G. 2016. Evolution of a Planar Wake in Adverse Pressure Gradient. *NASA/TM-2016-219068*.
- [3] Tummers, M.J., Passchier, D.M., Bakker, P.G. 2007. Experiments on the turbulent wake of a flat plate in a strong adverse pressure gradient. *Int. J.Heat and Fluid Flow*, **28**, 145-160.
- [4] Hoffenberg, R., Sullivan, J.P. 1998. Measurement and simulation of wake deceleration. *AIAA Paper 98-0522*.
- [5] Shur, M.L., Spalart, P.R., Strelets, M.Kh, Travin, A.K. 2008. A hybrid RANS-LES approach with delayed-DES and wall-modelled LES capabilities. *Int. J. Heat and Fluid Flow*, **29**, 1638-1649.
- [6] Shur, M.L., Spalart, P.R., Strelets, M.Kh, Travin, A.K. 2014. Synthetic Turbulence Generators for RANS-LES Interfaces in Zonal Simulations of Aerodynamic and Aeroacoustic Problems. *Flow, Turbulence and Combustion*, **93**, 63-92.
- [7] Menter, F.R. 1994. Two-Equation Eddy-Viscosity Turbulence Models for Engineering Applications. *AIAA Journal*, **32**, 1598–1605.
- [8] Shur, M., Strelets, M., Travin, A. 2018. Acoustically adapted versions of STG. *Notes Num. Fluid Mech. and Multidisciplinary Design*, **134**, 62-69.
- [9] Allmaras, S.R., Johnson, F.T., Spalart, P.R. 2012. Modifications and Clarifications for the Implementation of the Spalart-Allmaras Turbulence Model. *7th Int. Conf. on CFD - ICCFD7*.
- [10] Eisfeld, B., Rumsey, C.L., Togiti, V. 2016. Verification and Validation of a Second-Moment-Closure Model. *AIAA Journal*, **54**, 1524-1541.
- [11] Shur, M., Strelets, M. and Travin, A., High-order implicit multi-block Navier-Stokes code: Ten-years experience of application to RANS/DES/LES/DNS of turbulent flows. http://cfd.spbstu.ru/agarbaruk/c/document_library/DLFE-42505.pdf
- [12] Schwamborn, D., Gerhold T., Heinrich, R. 2006. The DLR TAU Code: Recent Applications in Research and Industry. *European Conf. on Comput. Fluid Dyn. ECCOMAS CFD-2006*.
- [13] Dejoan, A., Leschziner, M.A. 2005. Large eddy simulation of a plane turbulent wall jet. *Phys. Fluids*, **17**, 025102.